Radiocarbon, Vol 56, Nr 3, 2014, p 1175–1188 DOI: 10.2458/56.17771
© 2014 by the Arizona Board of Regents on behalf of the University of Arizona

A NUMERICAL EXAMINATION OF $^{14}CO_2$ CHAMBER METHODOLOGIES FOR SAMPLING AT THE SOIL SURFACE

Jocelyn Egan[1] • Nick Nickerson[2] • Claire Phillips[3] • Dave Risk[1]

ABSTRACT. Radiocarbon is an exceptionally useful tool for studying soil-respired CO_2, providing information about soil carbon turnover rates, depths of production, and the biological sources of production through partitioning. Unfortunately, little work has been done to thoroughly investigate the possibility of inherent biases present in current measurement techniques, like those present in $\delta^{13}CO_2$ methodologies, caused by disturbances to the soil's natural diffusive regime. This study investigates the degree of bias present in four ^{14}C sampling chamber methods using a three-dimensional numerical soil-atmosphere CO_2 diffusion model. The four chambers were tested in an idealized, surrogate reality by assessing measurement bias with varying $\Delta^{14}C$ and $\delta^{13}C$ signatures of production, collar lengths, soil biological productivity rates, and soil diffusivities. The static and Iso-FD chambers showed almost no isotopic measurement bias, significantly outperforming dynamic chambers, which demonstrated biases up to 200‰ in some modeled scenarios. The study also showed that ^{13}C and ^{14}C diffusive fractionation are not a constant multiple of one another, but that the $\delta^{13}C$ correction still works in diffusive scenarios because the change in fractionation is not large enough to impact measured $\Delta^{14}C$ values during chamber equilibration.

INTRODUCTION

The radioactive isotope of carbon (^{14}C) is an exceptionally useful tool for studying soil-respired CO_2, providing information about the biological sources of production through partitioning (Gaudinski et al. 2000; Trumbore 2000; Hahn et al. 2006; Schuur and Trumbore 2006; Hicks Pries et al. 2013). In recent years, many studies have utilized partitioning techniques, both physical and isotopic, as tools for separating sources of soil respiration, to understand how soil respiration sources may be affected by the future changing climate (Hanson et al. 2000; Högberg et al. 2001; Singh et al. 2003; Lee et al. 2003; Kuzyakov 2006; Moyes et al. 2010; Bond-Lamberty et al. 2011; Drake et al. 2012; Gomez-Casanovas et al. 2012; Risk et al. 2012). Source partitioning with isotopes has an advantage over physical partitioning as it is typically involves less disturbance than physical partitioning. However, in natural abundance isotopic partitioning studies, ^{14}C can be a more sensitive tool than $\delta^{13}C$. The difference between autotrophic and heterotrophic $\delta^{13}C$ signatures of soil-respired CO_2 is only a few permil (‰) (except in C_3-C_4 vegetation shifted studies), whereas there can be a much larger separation between $\Delta^{14}C$ source signatures, especially in systems where slow decomposition or long-term storage accentuate isotopic differences (Trumbore 2006). A peak in atmospheric $\Delta^{14}C$ signatures in 1963 caused by nuclear weapons testing has allowed researchers to utilize ^{14}C as a tracer to distinguish whether carbon substrates were utilized pre- or post-bomb, because post-bomb signatures are distinctive given their relative ^{14}C enrichment (Levin and Hesshaimer 2000). Autotrophic respiration consumes new carbon, so its ^{14}C signature will reflect current atmospheric $^{14}CO_2$ signatures, whereas heterotrophic signatures will reflect the age of the substrates that the heterotrophs consume, which can be very new or quite old (Gaudinski et al. 2000; Phillips et al. 2013).

Despite the potential utility of $^{14}CO_2$ as a tool for investigating soil-respired CO_2, little work has been done to thoroughly investigate the possibility of biases inherent to existing measurement techniques, because the high cost of analysis naturally drives researchers to focus effort on the ecological aspect of studies, rather than error or uncertainty testing. In the case of $\delta^{13}C$, Cerling et al. (1991) demonstrated that although mass differences in ^{12}C and ^{13}C isotopologues cause ^{12}C to diffuse 1.0044 times faster through the soil, if the soil is at a diffusive steady-state, the $\delta^{13}C$ of production should match the $\delta^{13}C$ of surface flux. Soils are, however, rarely at a diffusive steady-state, and

1. Dept. of Earth Sciences, St. Francis Xavier University, 1 West Street, Antigonish, Nova Scotia B2G 2W5, Canada. Corresponding author. Email: jegan@stfx.ca.
2. Dept. of Earth Sciences, Dalhousie University, 1459 Oxford Street, Halifax, Nova Scotia B3H 4R2, Canada.
3. Dept. of Crop and Soil Science, Oregon State University, Corvallis, Oregon 97331, USA.

https://doi.org/10.2458/56.17771 Published online by Cambridge University Press

research looking at $\delta^{13}C$ has shown that non-steady-state transport fractionations can be induced by soil transport (Nickerson and Risk 2009a; Moyes et al. 2010) and headspace sampling (Ohlsson 2010), where non-steady-state chambers can induce a bias of 4‰ and steady-state chambers up to 15‰ caused by lateral diffusion (Nickerson and Risk 2009b). The magnitude of these biases could potentially overprint the $\delta^{13}CO_2$ signatures of biological flux (Kayler et al. 2010; Moyes et al. 2010; Phillips et al. 2010), making partitioning difficult. These time-dependent fractionations ("dynamic fractionations"; Nickerson and Risk 2009a) will also be present and will potentially cause biases when attempting to measure $^{14}CO_2$, because like $^{13}CO_2$, $^{14}CO_2$ has a different diffusion coefficient than $^{12}CO_2$, diffusing 1.0088 times slower (Wang et al. 1994). Currently, to calculate $\Delta^{14}C$, researchers use $\delta^{13}C$ to correct for potential steady-state mass-dependent fractionations (Stuiver and Polach 1977). The $\delta^{13}C$ correction will not account for dynamic fractionations, however, because the assumption that ^{14}C fractionation is a constant multiple of ^{13}C fractionation may not hold in typical measurement conditions where the soils are rarely at steady-state. It will therefore be of interest to the ^{14}C community to know if steady-state and non-steady-state chamber methods used to measure $\Delta^{14}C$ of soil-respired CO_2 induce bias in a similar magnitude to those of $\delta^{13}C$.

In order for researchers to understand bias that may have been induced by $^{14}CO_2$ chamber methodologies in past studies, and to help decide which chamber method is the most robust for future studies, we utilized a three-dimensional numerical soil-atmosphere model to simulate soil-atmosphere-chamber exchange of CO_2 isotopologues, including $^{14}CO_2$, to compare isotopic signatures measured by various chamber methods to the natural steady-state. We also examined the effect of chamber-specific protocols, such as pump speed, stable isotopic signature calculations, and mixing model type, to determine the effect of these on the final estimates of stable and radioactive isotopic signature. Additionally, we investigated whether $\Delta^{14}C$ of soil flux changed during equilibration, and the amount by which $^{13}CO_2$ and $^{14}CO_2$ fractionation factors differ from one another during chamber equilibration. This was done in order to understand whether a biased stable isotopic value for flux used as a correction in the calculation of $\Delta^{14}C$ will affect the results. We predict that static and dynamic chambers will induce more bias measuring $\Delta^{14}C$ of flux than they do for $\delta^{13}C$, as the diffusive fractionation factor for $^{14}CO_2$ is larger (Stuiver and Polach 1977), and furthermore because additional error could be related to the $\delta^{13}C$ correction in a dynamic environment.

METHODS

Soil-Atmosphere Model

A three-dimensional coupled soil-atmosphere-chamber model was used to explore biases inherent in current $^{14}CO_2$ chamber methodologies. The model simulates CO_2 produced in the soil, diffusion to the atmosphere, and in some cases into a chamber on the surface of the modeled soil. Model physics and structure are further described in Creelman et al. (2013); the present version of the model adds $^{13}CO_2$ and $^{14}CO_2$ functionality in addition to $^{12}CO_2$.

Diffusion of each carbon isotopologue of CO_2 ($^{12}CO_2$, $^{13}CO_2$, and $^{14}CO_2$) is modeled according to Fick's law with its own specific atmospheric concentration, production, and diffusion rate. The simulations described here build on related work by Risk and Kellman (2008) and Nickerson and Risk (2009b), which used similar Fick's law–based models to examine the impacts of non-steady-state conditions on the soil surface flux of stable C isotopologues of CO_2. The model reproduces patterns of atmospheric invasion and soil air enrichment described in seminal papers on natural steady-state soil isotopic composition (Cerling et al. 1991; Wang et al. 1994; Davidson 1995; Amundson et al. 1998). The use of numerical simulation allows us to address both steady-state and time-dependent (non-steady-state) system dynamics that are not encompassed in the analytical solutions presented

https://doi.org/10.2458/56.17771 Published online by Cambridge University Press

in the earlier research. Drivers of these non-steady-state dynamics include soils undergoing rapid day-night changes in respiration rate, wind-induced advection, or temporary disruption of the natural steady-state regime owing to emplacement of a chamber on the surface (Risk and Kellman 2008; Venterea and Baker 2008; Bowling et al. 2009; Nickerson and Risk 2009a,b; Kayler et al. 2010; Phillips et al. 2010; Creelman et al. 2013). These settings have been shown to induce transient fractionations that are not predicted by the steady-state literature.

The model assumes that radioactive decay is negligible for $^{14}CO_2$ over the timescale of the measurements (Cerling et al. 1991; Wang et al. 1994). We produced model runs for each isotopologue where the resulting concentrations and fluxes of each isotopic species are used to calculate total CO_2, $\delta^{13}C$, and $\Delta^{14}C$ signatures of the soil CO_2 and surface flux at each time step.

Simulations were performed using a set of soil production rates, soil diffusivity coefficients, chamber collar lengths (downward extent of the collar below the soil), and $\delta^{13}C$ and $\Delta^{14}C$ signatures of biological production (Table 1). In all model scenarios, the $\delta^{13}C$ and $\Delta^{14}C$ of the atmosphere were 8.8‰ and 100‰, respectively, which are in the range of most typical environments.

Table 1 Model parameters.

Variable	Ranges
Diffusivity (m^2/s)	10^{-8}, 5×10^{-8}, 10^{-7}, 5×10^{-7}, 10^{-6}, 5×10^{-6}
Productivity ($\mu mol/m^2/s$)	0.1, 1, 5
Collar length (cm)	0, 2, 4, 8
$\delta^{13}C$ of production (‰)	–30, –20, –15
$\Delta^{14}C$ of production (‰)	–500, –200, 0, 200, 500

Calculation of Isotopic Signatures

The model output calculates isotopic signatures using delta notation. $\delta^{13}C$ is presented in ‰ as

$$\delta^{13}C = \left(\left(R_s \middle/ R_{std}\right) - 1\right) \times 1000 \tag{1}$$

where R_s is the $^{13}C/^{12}C$ ratio of the sample and R_{std} is the $^{13}C/^{12}C$ ratio of the PDB standard. For radiocarbon, $\Delta^{14}C$ is also presented in ‰ using the value of fraction modern (FM) of the sample:

$$\Delta^{14}C = \left(FM - 1\right) \times 1000 \tag{2}$$

FM is calculated using A_s, the measured activity of the sample, where the model outputs a $^{14}C/^{12}C$ ratio, which is equivalent to A_s to the fourth decimal place (Southon 2011). A_{abs} is the measured activity of the oxalic acid standard, with a model parameterization value of $1.2511e^{-12}$, where A_{abs} is 0.95 times the activity of the oxalic acid standard in 1950, corrected to a $\delta^{13}C$ of –19‰ (Stuiver and Polach 1977):

$$FM = \frac{\left(\frac{A_s}{A_{abs}}\right)\left(1 - \frac{25}{1000}\right)^2}{\left(1 + \frac{\delta^{13}C_s}{1000}\right)^2} \tag{3}$$

https://doi.org/10.2458/56.17771 Published online by Cambridge University Press

where $\delta^{13}C_s$ is the $\delta^{13}C$ signature of the sample, and 25 is the sample activity corrected for $\delta^{13}C$ isotopic fractionation.

Chamber Descriptions

Four chambers utilized in previous studies were simulated, and are described below and represented graphically in Figure 1. All calculations to determine chamber $\delta^{13}C$ and $\Delta^{14}C$ from the model output were performed using the equations provided in the original studies. All results were converted to $\Delta^{14}C$ notation in cases where the results were calculated in percent modern or fraction modern, to facilitate comparison of the results between different chambers.

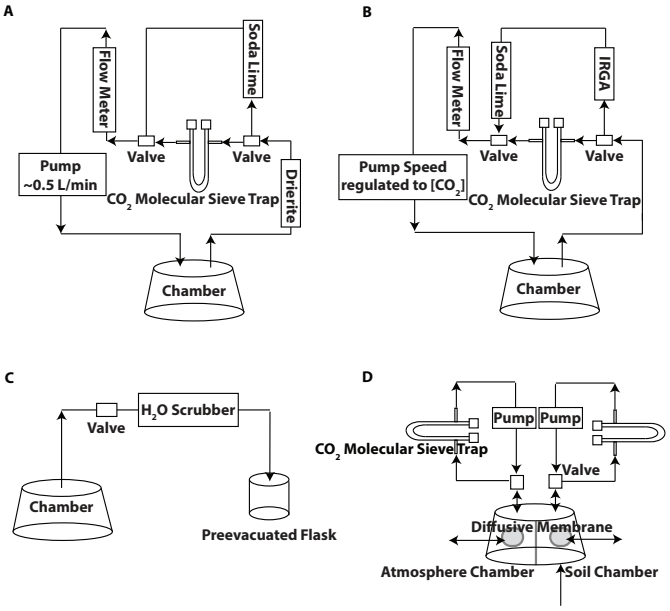


Figure 1 The four chambers that were modeled: (A) A dynamic chamber with a pump speed set to 0.5 L/min (Gaudinski et al. 2000); (B) A dynamic chamber with a pump speed that matches the flux rate (Schuur and Trumbore 2006); (C) A static chamber where CO_2 accumulates for 30 min prior to sampling (Hahn et al. 2006); (D) A diffusion-driven dynamic chamber, which is based on the isotopic-forced diffusion (Iso-FD) design for a $\delta^{13}C$ chamber presented in Nickerson et al. (2013).

Dynamic Chambers

Dynamic chambers are a type of steady-state chamber often employed in soil flux studies, including ^{14}C studies. They theoretically minimize alteration to the soil CO_2 concentration gradient by flowing atmospheric air or a CO_2-free gas through the chamber, which decreases the headspace concentration in order to maintain chamber concentrations closer to the surrounding atmosphere (Rayment and Jarvis 1997). We chose two dynamic chambers to model. Chamber A has a volume of ~11.5 L and is based on the chamber presented in Gaudinski et al. (2000). It utilized a pump with a constant flow rate of 0.5 L/min, and soda lime column to decrease the headspace concentration, regardless of the soil flux value at the time of measurement, just before diverting the flow path into a molecular sieve trap to collect 2 mg C for ^{14}C analysis. For modeling purposes, we assumed that the soda lime and molecular trap were perfectly efficient at removing CO_2 from the air stream, and further, that there was no isotopic fractionation associated with either process. Stable isotopic ($\delta^{13}C$) signatures of surface flux were used to correct the $\Delta^{14}C$ of the headspace for mass-dependent fractionation and for incomplete stripping of atmospheric CO_2 during the trapping period using the following equation:

$$X = \frac{\delta^{13}C_{measured} - \delta^{13}C_{soil}}{\delta^{13}C_{atmosphere} - \delta^{13}C_{soil}} \quad (4)$$

https://doi.org/10.2458/56.17771 Published online by Cambridge University Press

where X is the fraction of remnant atmospheric air in the sample, $\delta^{13}C_{atmosphere}$ is the atmospheric $\delta^{13}C$ signature, and $\delta^{13}C_{soil}$ is the $\delta^{13}C$ signature of soil respiration. $\Delta^{14}C$ is then calculated as

$$\Delta^{14}C_{soil} = \frac{\Delta^{14}C_{measured} - X \times \Delta^{14}C_{atmosphere}}{1 - X} \quad (5)$$

Chamber B differs from Chamber A by using an infrared gas analyzer in-line with the pump to determine the flux rate into the headspace prior to CO_2 scrubbing. The pump speed was adjusted to match the soil flux rate, thereby maintaining near natural steady-state conditions in the chamber (Schuur and Trumbore 2006). The same equations for X and $\Delta^{14}C_{soil}$ that were used for Chamber A were also used for Chamber B. The modeled volume (11.5 L) and surface area (0.058 m^2) of Chamber B were based on the values used in Schuur and Trumbore (2006).

Static Chamber

Static chambers are a type of non-steady-state chamber in which CO_2 from soil is allowed to accumulate without interference in the chamber headspace. In the case of ^{14}C sampling, after the accumulation period, a molecular sieve trap or sampling flask captures gas from the headspace. For modeling scenarios, the static chamber, Chamber C, is based on the one presented by Hahn et al. (2006). The chamber was deployed for 30 min to allow CO_2 accumulation in the headspace before sampling, thereby ensuring that enough CO_2 is captured in the sampling flask for $\Delta^{14}C$ analysis. For consistency, we also modeled this chamber with a volume of 11.5 L. Isotopic signatures ($\delta^{13}C$ and $\Delta^{14}C$) of flux were calculated using a standard two-source mixing model:

$$\delta^{13}C_{respired} = \frac{\delta^{13}C_{chamber} \times [CO_2]_{chamber} - \delta^{13}C_{freeair} \times [CO_2]_{freeair}}{[CO_2]_{chamber} - [CO_2]_{freeair}} \quad (6)$$

where $\delta^{13}C_{respired}$ is the stable isotopic signature of respired CO_2, $\delta^{13}C_{chamber}$ and $[CO_2]_{chamber}$ are the stable isotopic signature and CO_2 concentration of chamber air, respectively, and $\delta^{13}C_{freeair}$ and $[CO_2]_{freeair}$ are the stable isotopic signature and CO_2 concentration of the free air (near-surface atmosphere). A similar equation can be constructed to calculate the chamber estimate respired ^{14}C activity, which can then be converted to the $\Delta^{14}C$ signature (Hahn et al. 2006).

Isotopic-Forced Diffusion Chamber

The isotopic-forced diffusion (Iso-FD) chamber is similar in design to a dynamic chamber, but rather than mass outflow, the air exchange between the chamber and atmosphere is regulated by a diffusive membrane (Figure 1D). This chamber design has been tested as a tool for sampling $\delta^{13}CO_2$ (Nickerson et al. 2013) and is based on the forced diffusion (FD) bulk CO_2 flux chamber presented by Risk et al. (2011). Here, we evaluated its theoretical performance for $\Delta^{14}C$ sampling (Chamber D). The principle of FD operation is to restrict exchange between the chamber and the atmosphere passively using membranes of known diffusivities. The offset in CO_2 concentration and isotopic abundance between the chamber and the surrounding atmosphere can then be related to soil flux rate and composition. Membranes of particular diffusivities and panel surface areas were chosen for the specific chamber geometry in order to obtain the ideal amount of CO_2 buildup in the chamber for measurements with the smallest error (Creelman et al. 2013). As is the case with the dynamic chamber, FD chamber interior concentrations are an intermediate between the atmosphere and soil, so the technique uses an atmospheric reference chamber, which has no soil inlet, alongside the FD chamber, to correct for changes in the atmospheric concentrations in the mass balance equation. For this configuration, both the chamber and atmospheric reference were coupled to molecular

https://doi.org/10.2458/56.17771 Published online by Cambridge University Press

sieve traps. $\Delta^{14}C$ signatures were calculated from the model output for this chamber using the following equation, modified from that presented in Nickerson et al. (2013):

$$\frac{F_{in}^{14C}}{F_{in}^{12C}} = \frac{1}{1.0088}\frac{(C_{FD}^{14C} - C_{atm}^{14C})}{(C_{FD}^{12C} - C_{atm}^{12C})} \quad (7)$$

where $F_{in}^{14C} / F_{in}^{12C}$ is equivalent to A_s and can be represented in delta notation with Equations 2 and 3, 1.0088 is the diffusive fractionation factor for $^{14}CO_2$ (Wang et al. 1994), and C_{FD} and C_{atm} are the concentrations of each isotopologue present in the Iso-FD chamber and atmospheric reference chamber. Again, for consistency the modeled volume and surface area of the chamber were 11.5 L and 0.058 m^2, respectively.

Error Analysis

Propagation of uncertainty (error) was calculated for the chambers using the standard partial derivative form (Ku 1966):

$$S_f = \sqrt{\left(\frac{\partial f}{\partial x}\right)^2 S_x^2 + \left(\frac{\partial f}{\partial y}\right)^2 S_y^2 + \left(\frac{\partial f}{\partial z}\right)^2 S_z^2 + \ldots} \quad (8)$$

where s_f is the absolute error in the function f, which is composed of the variables x, y, z, and so on, each with variable specific uncertainty s_x, s_y, s_z. For the specific equations used for each chamber, see Appendices A and B in the online Supplementary material.

RESULTS AND DISCUSSION

Dynamic Chambers (A and B)

Simulations of Chamber A, which used a constant pump speed of 0.5 L/min, showed that headspace CO_2 concentrations could differ substantially from the atmosphere unless the soil flux rates were well matched to the CO_2 scrubbing rates. Assuming steady-state concentrations at the soil surface were initially in the range of about 380–1000 ppm CO_2, using a constant pump speed of 0.5 L/min, the optimal soil flux rate into the chamber should have been 2–6 μmol m^{-2} s^{-1} in order to maintain steady-state concentrations. When soil flux rates fell in this range, our simulation results showed ^{14}C errors were at their lowest (Figure 2A). This suggested that the main driver of error for Chamber A is the constant pump rate, which is unable to maintain a near steady-state concentration during measurement when fluxes are too low or too high to match the rate of CO_2 removal.

$\Delta^{14}CO_2$ errors were exacerbated when Chamber A was placed on virtual porous soils, and where flux rates were low (Figure 2A). This was due to a combination of overpumping and lateral diffusion, a problem that is exacerbated in soils of high soil diffusivity. In low-diffusivity soils, however, the chamber performed relatively well because of the limited feedback between the chamber and the soil, which created an effective 1D diffusion pathway eliminating lateral diffusion errors. Results from simulations with varying soil collar depth helped support the interpretation that lateral diffusion contributed to ^{14}C measurement errors. When the collar depth was increased at fixed levels of diffusivity and production, $\Delta^{14}C$ errors decreased linearly (data not shown).

The apparent ^{14}C errors associated with Chamber A were also affected by similarity in isotopic values of soil CO_2 production and atmospheric CO_2. This increase in bias arose because of the chamber-based errors in the estimate of X (Equation 4). Any error in the chamber estimate becomes amplified because the two $\delta^{13}C$ values are differenced in the denominator of the calculation. As the

https://doi.org/10.2458/56.17771 Published online by Cambridge University Press

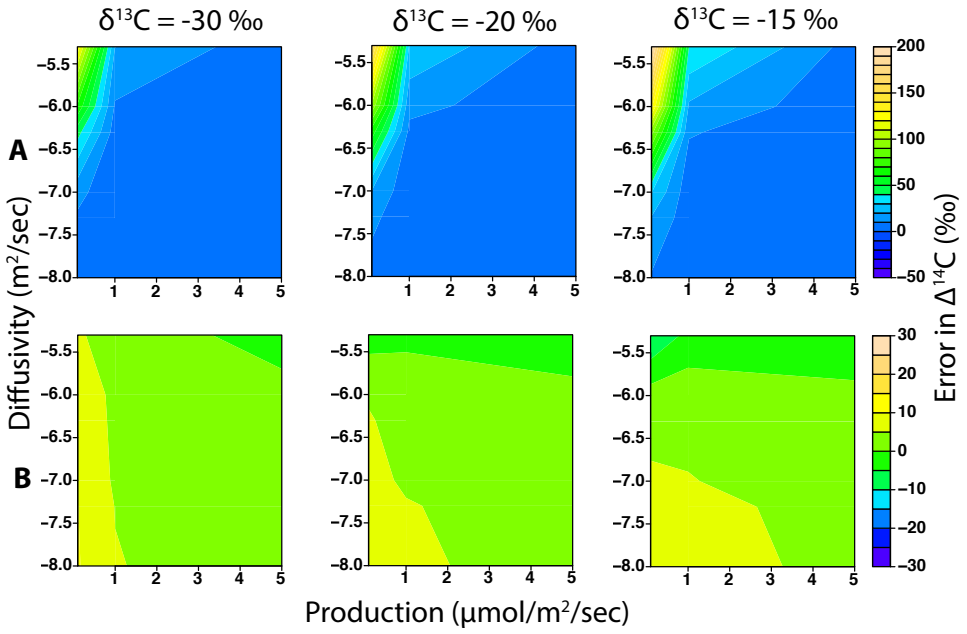


Figure 2 Contour plots of model output error of $\Delta^{14}C$ (‰) of Chamber A (panel A) and Chamber B (panel B) with a simulated $\Delta^{14}C$ of production of –200‰, collar length of 2 cm, and $\delta^{13}C$ of production of –30‰, –20‰, and –15‰ in columns 1, 2 and 3, respectively. Soil production (µmol/m^2/s) is on the *x* axis and soil diffusivity (log-scaled where axis numbers are 10^y; m^2/s) on the *y* axis. Note the scale differences between Chamber A and Chamber B.

$\delta^{13}C$ signature of production became more enriched, overestimates in $\Delta^{14}C$ began to appear in lower porosity soils (i.e. soils with higher moisture/bulk density). Similarly, biases also became larger in porous soils with low biological productivity (Figure 2A).

When the specified $\Delta^{14}CO_2$ of production in the model was more enriched, in porous soils with low fluxes, the chamber-measured signatures were more depleted than they should have been. When the signatures of production were more depleted, the chamber yielded more enriched values than it should have (Figure 3A). Near the point where soil production and atmospheric $\Delta^{14}CO_2$ were similar, the error in measurement was minimized. This minimized error was likely an *apparent* minima caused by the lack of distinction between source and ambient $\Delta^{14}CO_2$ signatures.

For Chamber B, in which pump speed was regulated to hold CO_2 at a constant concentration, modeled errors varied with soil porosity and productivity. In soils with high diffusivity, $\Delta^{14}CO_2$ was slightly underestimated, and slightly overestimated in soils with low diffusivities and low biological production rates. The adjustment of the pump speed to the ambient atmospheric concentration led to the maintenance of near steady-state concentrations in the chamber during the measurement period, with some deviation from the true steady-state caused by soil diffusivity (and therefore soil collar length) and the slight stratification of the model atmosphere, causing the slight over- and underestimates.

Similar to the Chamber A results, if the $\delta^{13}C$ signature of production and atmosphere were considerably different, $\Delta^{14}CO_2$ deviations from the true isotopic value occurred in soils with low productivity. However, as the $\delta^{13}C$ signature of production approached that of the atmosphere (more enriched), deviations similarly became apparent in highly productive soils (Figure 2B). In soils when the $\Delta^{14}CO_2$ of production was depleted relative to the atmosphere, Chamber B gave slight overestimates of $\Delta^{14}CO_2$. If the $\Delta^{14}CO_2$ of production were to be enriched more than the range of our

https://doi.org/10.2458/56.17771 Published online by Cambridge University Press

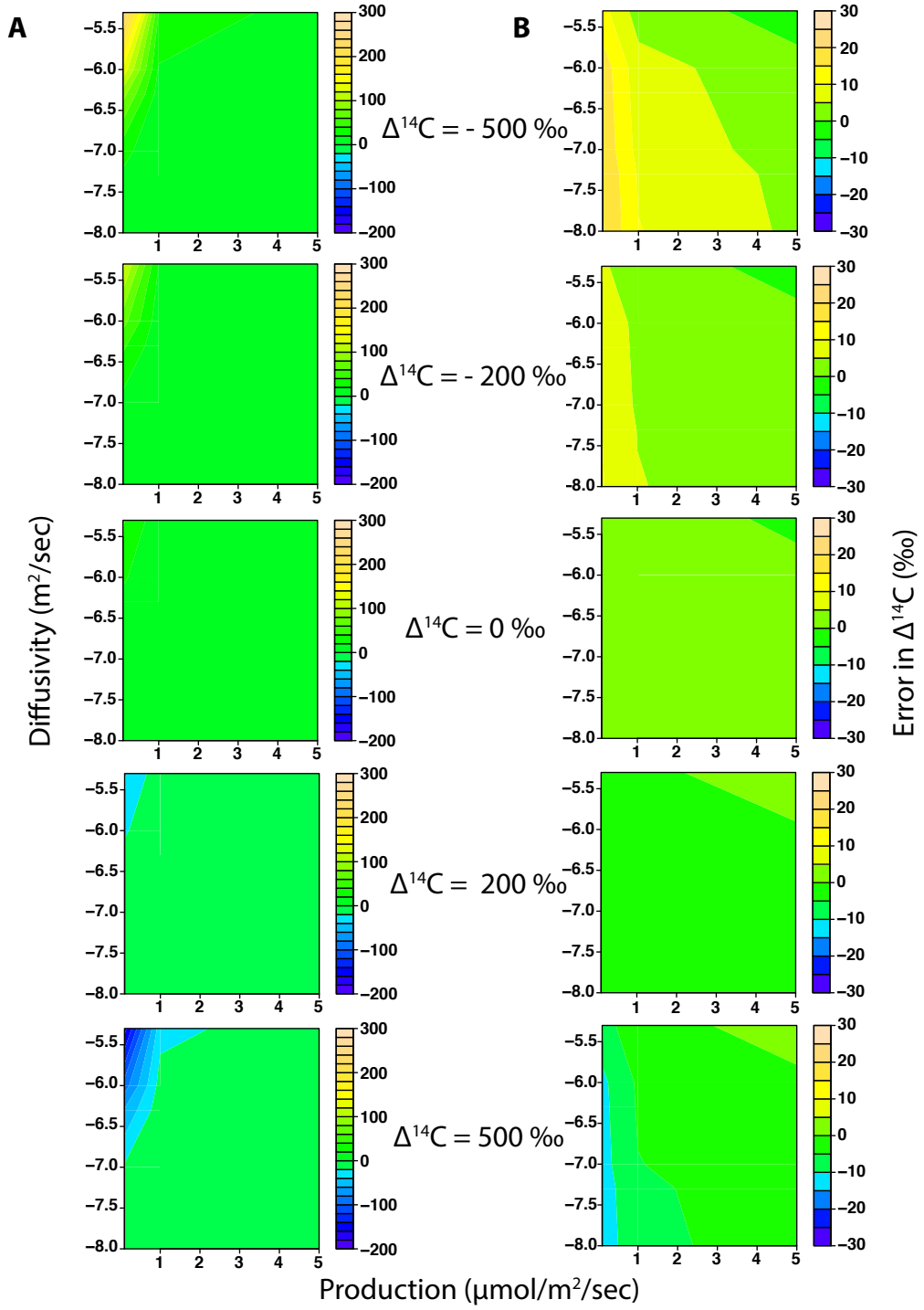


Figure 3 Contour plots of model output error of $\Delta^{14}C$ (‰) of Chamber A (column A) and Chamber B (column B) with a simulated $\delta^{13}C$ of production of –30‰, collar length of 2 cm, and $\Delta^{14}C$ of production of –500‰, –200‰, 0‰, 200‰, and 500‰ in rows 1, 2, 3, 4, and 5 respectively. Soil production (μmol/m^2/s) is on the *x* axis and soil diffusivity (log-scaled where axis numbers are 10^y; m^2/s) on the *y* axis. Note the scale differences between Chamber A and Chamber B.

https://doi.org/10.2458/56.17771 Published online by Cambridge University Press

model simulations, the chamber would produce slight underestimates across all diffusivities, again in soils with lower productivity (Figure 3B).

Error analysis performed on Chamber A and B provided further explanation for deviations in isotopic signature when the prescribed isotopic signature of production was similar to that of the atmosphere. Uncertainty estimates for the dynamic chambers consist of two necessary calculations, the first of which is the uncertainty in *X*, the fraction of remaining atmospheric air in the chamber. Uncertainty in *X* is largely driven by the difference between $\delta^{13}C_{atm}$ and $\delta^{13}C_{soil}$ (the denominator in Equation 4), where large differences between the two values minimize the error. Shown in Figure 4a are uncertainty estimates in *X* (unitless) as a function of $\delta^{13}C_{atm}$ and $\delta^{13}C_{soil}$ for measurement errors of 0.1‰ (open squares) in all of the variables in Equation 4, and 0.3‰ measurement error in $\delta^{13}C_{atmosphere}$ and $\delta^{13}C_{measured}$ and 1.0‰ measurement error in $\delta^{13}C_{soil}$ (circles).

Figure 4b shows the subsequent $\Delta^{14}C_{soil}$ uncertainty estimates as a function of *X* for measurement errors of 10‰ in $\Delta^{14}C_{measured}$ and $\Delta^{14}C_{atmosphere}$, and error in *X* of 0.01, displayed in the open squares. While the value of *X* drives the largest uncertainty in the estimate of $\Delta^{14}C_{soil}$, the spread in the uncertainty data at a given *X* value is linearly related to the absolute difference between $\Delta^{14}C_{measured}$ and $\Delta^{14}C_{atmosphere}$. Also shown is the uncertainty for measurement errors of 50‰ in $\Delta^{14}C_{measured}$ and $\Delta^{14}C_{atmosphere}$, and error in *X* of 0.1 (gray circles).

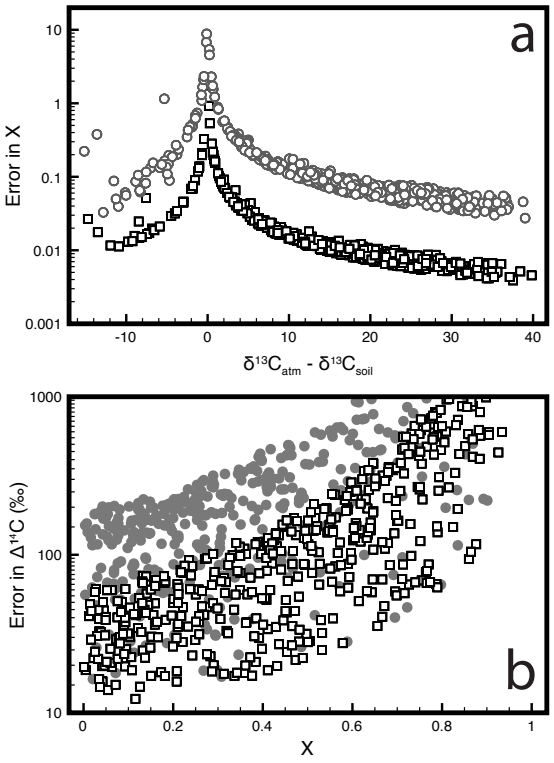


Figure 4 Uncertainty estimates for the dynamic chambers. (a) Uncertainty estimates in *X*, the fraction of remaining atmospheric air in the chamber (unitless), as a function of $\delta^{13}C_{atm}$ and $\delta^{13}C_{soil}$ for measurement errors of 0.1‰ in all of the variables in Equation 4 (open squares), and 0.3‰ measurement error in $\delta^{13}C_{atmosphere}$ and $\delta^{13}C_{measured}$ and 1.0‰ measurement error in $\delta^{13}C_{soil}$ (circles). (b) $\Delta^{14}C_{soil}$ uncertainty estimates as a function of *X* for measurement errors of 10‰ in $\Delta^{14}C_{measured}$ and $\Delta^{14}C_{atmosphere}$, and error in *X* of 0.01 (open squares), and the uncertainty for measurement errors of 50‰ in $\Delta^{14}C_{measured}$ and $\Delta^{14}C_{atmosphere}$, and error in *X* of 0.1 (gray circles).

Based on the uncertainty analysis, measurements of $\Delta^{14}C$ done with a dynamic chamber can be made with much more certainty in scenarios where the atmosphere values of $\delta^{13}C$ and $\Delta^{14}C$ are different (5‰ in the case $\delta^{13}C$) from the $\delta^{13}C$ and $\Delta^{14}C$ of the soil.

As demonstrated through the comparison of Chambers A and B in Figures 2 and 3, Chamber B per-

https://doi.org/10.2458/56.17771 Published online by Cambridge University Press

formed consistently better than Chamber A in all simulated scenarios. We attribute this increased performance to maintenance of near steady-state conditions through the adjustment of pump speed. With a constant pump speed, there is an optimal range of flux rates when Chamber A can perform well, but it is less applicable than Chamber B across a large range of soil conditions.

Static Chamber (C)

Previous numerical modeling by Nickerson and Risk (2009b) showed a bias towards underestimation of $\delta^{13}CO_2$ using static chamber designs. The combination of a strong concentration gradient between the soil and chamber, and diffusive fractionation caused $^{12}CO_2$ to accumulate in the chamber before $^{13}CO_2$, and tended to make the signature of the chamber headspace more negative than the equilibrium condition, as $^{13}CO_2$ caught up (see Figure 3 of Nickerson and Risk 2009b). We expected to see similar results when this type of chamber was used to measure $^{14}CO_2$, but did not. In fact, the static chamber design (Chamber C) performed very well over the whole range of soil conditions, with the deviation from the true isotopic signature of $\Delta^{14}CO_2$ flux being in the numerical error bounds of the model (~1‰ $\Delta^{14}CO_2$).

Based on subsequent analytical modeling of the chamber isotopic signatures (data not shown), it seems that the marginally increased fractionation factor for $^{14}CO_2$ (1.0044 for $^{13}CO_2$ and 1.0088 for $^{14}CO_2$) is balanced by a very low $^{14}CO_2$ concentration gradient, leading to a smooth transition from atmospheric to respired isotopic signatures for $\Delta^{14}CO_2$. When the fractionation factor was increased in the analytical model, the nonlinear mixing behavior that was noted in the $\delta^{13}CO_2$ simulations became evident in the $\Delta^{14}CO_2$ results. Similarly, if the fractionation factor was held at 1.0088, but the absolute abundance of $^{14}CO_2$ increased, with $^{12}CO_2$ and $^{13}CO_2$ staying the same (and thus the gradients between soil and atmosphere became larger), the nonlinear mixing behavior also became evident.

Figure 5 shows the probable uncertainty for the static chamber. It assumes two error rates, the first with a measurement error of 10‰ (5‰ AMS error and 5‰ sampling and extraction error; Phillips et al. 2013) in $\Delta^{14}C$ signatures and 1% in bulk gas concentrations (open squares), and the second with measurement errors of 50‰ in $\Delta^{14}C$ signatures and 5% in bulk gas concentrations (open circles). Most of the uncertainty in the estimation of the ^{14}C fluxes with this chamber comes from the ratio of the final (C_2) and initial concentrations (C_1). Like the dynamic chambers, measurements made with the static chamber can be done with more certainty when the final chamber measurements are at least twice the value of the initial chamber measurements.

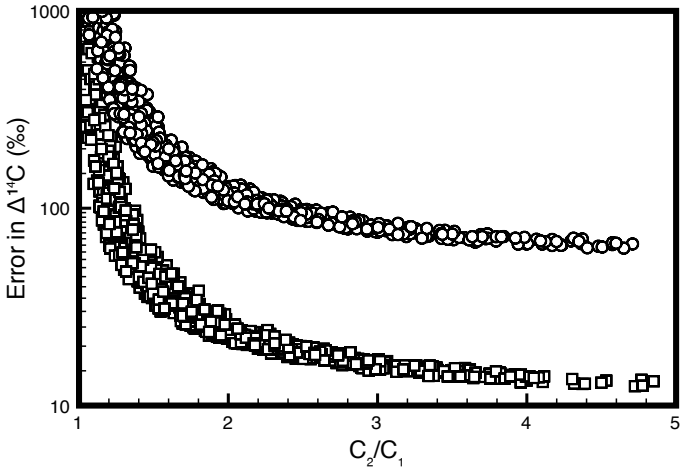


Figure 5 The probable uncertainty for static and Iso-FD chambers assuming two error rates, the first with a measurement error of 10‰ in $\Delta^{14}C$ signatures and 1% in bulk gas concentrations (open squares), and the second with measurement errors of 50‰ in $\Delta^{14}C$ signatures and 5% in bulk gas concentrations (open circles). C_1 and C_2 are the initial and final concentrations for the static chamber, or for the Iso-FD chamber, they are equivalent to the atmospheric chamber and soil chamber measurements.

https://doi.org/10.2458/56.17771 Published online by Cambridge University Press

Isotopic-Forced Diffusion Chamber (D)

In all simulations with the Iso-FD chamber, the predicted isotopic signature of flux was very near the prescribed value. Similar to the static chamber results, the Iso-FD results were within the numerical error bounds of the model (~1‰ $\Delta^{14}CO_2$). We attribute the accuracy of this chamber to the fact that a diffusive steady-state was maintained during the measurement period, avoiding isotopic disequilibrium created by other chamber designs. Simulations showed that the $\Delta^{14}CO_2$ behavior for this chamber is similar to that described in Nickerson et al. (2013) for $\delta^{13}CO_2$, where a slight build-up of concentration in the chamber headspace produced concentration and isotopic plumes directly below the chamber. However, despite these plumes, sampling errors were negligible.

Assuming the fractionation factor for the Iso-FD calculations is constant and known, the uncertainty for the Iso-FD chamber takes the same form as the static chamber and uses the same calculation variables (Figure 5). For the Iso-FD chamber, most of the uncertainty in the estimation of the ^{14}C fluxes comes from the ratio of concentration measurements in soil chamber and atmospheric chamber measurements, which can be thought of as equivalent to the ratio of the final (C_2) and initial concentrations (C_1) for the static chamber. As was the case with the dynamic chambers and static chamber, measurements made with Iso-FD chambers have more certainty when the soil chamber concentration measurements are at least twice the value of the atmospheric chamber measurements.

Other Considerations

There are also some other possible biases that should be considered, which are not included in the model. The simulated soil in the model is at steady-state. It has a constant biological production, soil diffusivity, and isotopic signature of production through depth, so no natural non-steady-state (NSS) effects (Nickerson and Risk 2009a) are included in the results. A nonuniform soil with varying diffusivities and production rates through depth would provide different model results than the uniform modeled soil (Venterea and Baker 2008). Nickerson and Risk (2009a) and Moyes et al. (2010) demonstrated the effects of dynamic fractionations, where soil features and processes such as biological production, diffusivity, pore space, and atmospheric concentrations, which have temporal variation, will induce NSS transport conditions that lead to transient changes in the isotopic composition of the soil CO_2 flux. The main driving force behind this is the difference in the diffusion rate between CO_2 isotopologues, which will be slightly amplified when considering $^{14}CO_2$ due to its increased mass. The measured values could therefore be further biased on top of the potential biases induced by the chamber method. Despite the counterbalance of low-^{14}C concentration gradients shown in the case of the static chamber, these dynamic fractionation effects should be investigated further in order to ensure that they are not causing bias.

The model also assumes that the method used to sample from the chamber, molecular sieve trap, or sampling flask is completely efficient and causes no fractionations. $\Delta^{14}C$ static chamber methods can include a capillary tube that attaches a sampling flask to the chamber (Hahn et al. 2006). This method could cause a potential fractionation, where the lighter isotopologue, $^{12}CO_2$, would travel faster than $^{14}CO_2$ through the capillary tube, so the resulting mixture in the sampling flask could potentially be more depleted than the mixture in the chamber headspace. It would be ideal to obtain a quick sample from the chamber, for example, by attaching the sampling flask under vacuum to the chamber and drawing 1 L of sample immediately. This configuration is similar to how the model simulates sampling from the chamber and would work well for the two-point mixing model used for static chambers (Hahn et al. 2006). Another issue not addressed in the model surrounding the static chamber and Iso-FD chamber methods is the possible stratification in the chamber headspace because of the lack of mixing. In the case of the static chamber, concentration stratification com-

https://doi.org/10.2458/56.17771 Published online by Cambridge University Press

bined with capillary tube errors could lead to an even greater bias in the captured gas in the sampling flask, where the gas traveling along the tube is not well mixed. For the Iso-FD chamber, there could also be problems with using molecular sieve traps, because as CO_2 is removed from the chamber headspace, it decreases the concentration in the chamber, causing the chamber to no longer be at steady-state. In the case of dynamic chambers, if the soda lime trap and molecular sieve trap have different trapping efficiencies, then the expected advantage of having a truer steady-state will not be met. If the soda lime and molecular sieve traps also fractionate ^{14}C, then the already biased results found in this study will be further biased.

Although the Iso-FD and static chambers perform well under all simulated conditions in the numerical model, there are some other things that need to be considered. The two samples needed for these chambers (soil or final chamber measurement, and atmosphere or initial chamber measurement) have to be different enough from one another, to keep the error rate within an acceptable range (Figure 6). For the Iso-FD chamber, this means choosing an appropriate membrane, and for the static chamber, this means leaving the chamber deployed for a long enough period of time. Therefore, in scenarios where the soil chamber or final concentrations and the atmospheric chamber or initial chamber concentrations are quite similar, these chambers would not be ideal.

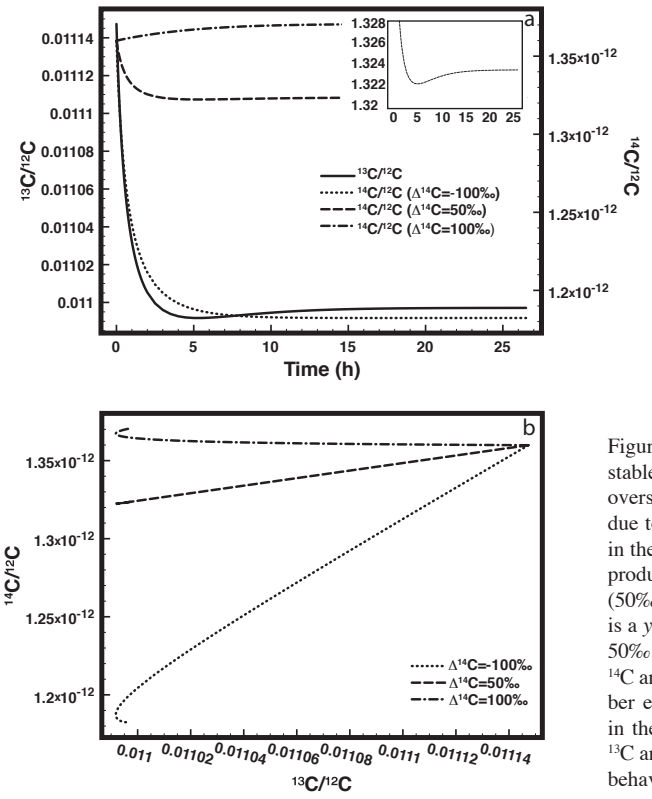


Figure 6 (a) Time series of chamber equilibration for stable carbon and ^{14}C ratios. Note that the $^{13}C/^{12}C$ ratio overshoots the equilibrium value between 2 and 10 hr due to lateral diffusion. This behavior is not present in the ^{14}C ratios except for when the ^{14}C signature of production and the ^{14}C signature of the atmosphere (50‰ for this model simulation) are equal. The insert is a *y*-axis zoom (*y*-axis values are 10^{-12}) of the $\Delta^{14}C$ 50‰ line to display the overshooting behavior. (b) ^{14}C and stable carbon ratio mixing lines during chamber equilibration for three $\Delta^{14}C$ signatures. A hook in the line signifies a different mixing behavior for ^{13}C and ^{14}C, whereas a straight line means the mixing behavior is the same for both isotopes.

The $\delta^{13}C$ correction used to account for mass-dependent fractionations in $\Delta^{14}C$ assumes that $^{14}CO_2$ and $^{13}CO_2$ diffusive fractionation are a constant multiple of one another. Figure 6 demonstrates that this assumption is incorrect. In a time series view of chamber equilibration (Figure 6a), $^{14}C/^{12}C$ does not behave in the same way as $^{13}C/^{12}C$ (lateral diffusion), except for when the ^{14}C signatures of production and atmosphere are equal (50‰ in this case). In Figure 6b, chamber equilibration mixing

https://doi.org/10.2458/56.17771 Published online by Cambridge University Press

lines of $^{14}C/^{12}C$ and $^{13}C/^{12}C$ demonstrate whether a difference in mixing between the stable and radioactive isotopes exists. A straight line shows that as ^{13}C increased in the chamber, ^{14}C increased in a constant proportion. A curvilinear line or hook, in contrast, shows that ^{14}C increased at a different rate than ^{13}C. Despite the differences in mixing behaviors between the isotopes (^{14}C fractionation is not a constant multiple of ^{13}C fractionation), the changes to the fractionation factor between the two isotopes that arises from lateral diffusion biases is not sufficient to have an impact on the ^{14}C result. In other words, the nonlinear behavior during chamber CO_2 accumulation is minor enough that assuming a fractionation for ^{14}C of twice ^{13}C fractionation produces errors far smaller than AMS error.

CONCLUSIONS

These model simulations suggested more favorable performance of soil surface sampling chambers than we expected. The static chamber had little sampling error in these simulations, whereas we expected it to have a greater bias than dynamic chambers, like in the case of $\delta^{13}C$ (Nickerson and Risk 2009b). Based on the simulation results, the static chamber and Iso-FD chamber performed the best under the range of soil conditions simulated. Other considerations should be made, however, when choosing a sampling method, including the choice between molecular sieve traps or sampling flasks, the cost, and the length of time needed to sample the chamber. This modeling exercise also showed that the assumption that stable and ^{14}C isotopic diffusion fractionations are a constant multiple of one another through time is not universally true, especially under non-steady-state conditions. The $\delta^{13}C$ correction still stands because the changes to the diffusive fractionation during equilibration are not large enough to impact $\Delta^{14}C$, but researchers should still be cautious, and this should be investigated further for non-steady-state soil conditions.

ACKNOWLEDGMENTS

This research was funded by Natural Sciences and Engineering Research Council (NSERC) through a CREATE grant to JE, and an NSERC PGS-D grant to NN. Computational resources were provided by ACEnet, the regional high performance computing consortium for universities in Atlantic Canada. Special thanks to Chance Creelman for his coding help.

REFERENCES

Amundson R, Stern L, Baisden T, Wang Y. 1998. The isotopic composition of soil and soil-respired CO_2. *Geoderma* 82(1–3):83–114.

Bond-Lamberty B, Bronson D, Bladyka E, Gower ST. 2011. A comparison of trenched plot techniques for partitioning soil respiration. *Soil Biology and Biochemistry* 43(10):2108–14.

Bowling DR, Massman WJ, Schaeffer SM, Burns SP, Monson RK, Williams MW. 2009. Biological and physical influences on the carbon isotope content of CO_2 in a subalpine forest snowpack, Niwot Ridge, Colorado. *Biogeochemistry* 95(1):37–59.

Cerling TE, Solomon DK, Quade J, Bowman JR. 1991. On the isotopic composition of carbon in soil carbon dioxide. *Geochimica et Cosmochimica Acta* 55(11): 3403–5.

Creelman C, Nickerson N, Risk D. 2013. Quantifying lateral diffusion error in soil CO_2 respiration estimates using numerical modeling. *Soil Science Society of America Journal* 77(3):699–8.

Davidson GR. 1995. The stable isotopic composition and measurement of carbon in soil CO_2. *Geochimica et Cosmochimica Acta* 59(12):2485–9.

Drake JE, Oishi AC, Giasson M-A, Oren R, Johnsen KH, Finzi AC. 2012. Trenching reduces soil heterotrophic activity in a loblolly pine (*Pinus taeda*) forest exposed to elevated atmospheric [CO_2] and N fertilization. *Agricultural and Forest Meteorology* 165:43–52.

Gaudinski JB, Trumbore SE, Davidson EA, Zheng S. 2000. Soil carbon cycling in a temperate forest: radiocarbon-based estimates of residence times, sequestration rates and partitioning fluxes. *Biogeochemistry* 51(1):33–69.

Gomez-Casanovas N, Matamala R, Cook DR, Gonzalez-Meler MA. 2012. Net ecosystem exchange modifies the relationship between the autotrophic and heterotrophic components of soil respiration with abiotic factors in prairie grasslands. *Global Change Biology* 18(8):2532–45.

Hahn V, Högberg P, Buchmann N. 2006. ^{14}C – a tool for separation of autotrophic and heterotrophic soil respiration. *Global Change Biology* 12(6):972–82.

Hanson PJ, Edwards NT, Garten CT, Andrews JA. 2000. Separating root and microbial contributions to soil respiration: a review of methods and observations. *Biogeochemistry* 48(1):115–48.

https://doi.org/10.2458/56.17771 Published online by Cambridge University Press

Hicks Pries CE, Schurr EAG, Crummer KG. 2013. Thawing permafrost increases old soil and autotrophic respiration in tundra: partitioning ecosystem respiration using $\delta^{13}C$ and $\Delta^{14}C$. *Global Change Biology* 19(2):649–61.

Högberg P, Nordren A, Buchmann N, Taylor A, Ekblad A, Högberg M, Nyberg G, Ottosson-Löfvenius M, Read D. 2001. Large-scale forest girdling shows that current photosynthesis drives soil respiration. *Nature* 411(6839):789–92.

Kayler Z, Sulzman E, Rugh W, Mix A, Bond B. 2010. Characterizing the impact of diffusive and advective soil gas transport on the measurement and interpretation of the isotopic signal of soil respiration. *Soil Biology and Biochemistry* 42(3):435–44.

Ku H. 1966. Notes on the use of propagation of error formulas. *Journal of Research of the National Bureau of Standards Section C: Engineering and Instrumentation* 70(4):263–73.

Kuzyakov Y. 2006. Sources of CO_2 efflux from soil and review of partitioning methods. *Soil Biology and Biochemistry* 38(4):425–48.

Lee M-S, Nakane K, Nakatsubo T, Koizumi H. 2003. Seasonal changes in the contribution of root respiration to total soil respiration in a cool-temperate deciduous forest. *Plant Soil* 255(1):311–8.

Levin I, Hesshaimer V. 2000. Radiocarbon—a unique tracer of global carbon cycle dynamics. *Radiocarbon* 42(3):69–80.

Moyes AB, Gaines SJ, Siegwolf RTW, Bowling DR. 2010. Diffusive fractionation complicates isotopic partitioning of autotrophic and heterotrophic sources of soil respiration. *Plant, Cell and Environment* 33(11):1804–19.

Nickerson N, Risk D. 2009a. Physical controls on the isotopic composition of soil respired CO_2. *Journal of Geophysical Research* 114(G1):G01013.

Nickerson N, Risk D. 2009b. A numerical evaluation of chamber methodologies used in measuring the $\delta^{13}C$ of soil respiration. *Rapid Communications in Mass Spectrometry* 23(17):2802–10.

Nickerson N, Egan J, Risk D. 2013. Iso-FD: a novel method for measuring the isotopic signature of surface flux. *Soil Biology and Biochemistry* 62:99–6.

Ohlsson KEA. 2010. Reduction of bias in static closed chamber measurements of $\delta^{13}C$ in soil CO_2 flux. *Rapid Communications in Mass Spectrometry* 24(2): 180–4.

Phillips CL, Nickerson N, Risk D, Kayler Z, Andersen C, Mix AC, Bond BJ. 2010. Soil moisture effects on the carbon isotope composition of soil respiration. *Rapid Communications in Mass Spectrometry* 24(9): 1271–80.

Phillips CL, McFarlane K, Risk D, Desai AR. 2013. Biological and physical influences on soil $^{14}CO_2$ seasonal dynamics in a temperate hardwood forest. *Biogeosciences Discussions* 10:10,721–58.

Rayment MB, Jarvis PG. 1997. An improved open chamber system for measuring soil CO_2 effluxes in the field. *Journal of Geophysical Research – Atmosphere* 102(D24):28,779–84.

Risk D, Kellman L. 2008. Isotopic fractionation in non-equilibrium diffusive environments. *Geophysical Research Letters* 35(2):L02403.

Risk D, Nickerson N, Creelman C, McArthur G, Owens J. 2011. Forced diffusion soil flux: a new technique for continuous monitoring of gas efflux. *Agricultural Forest Meteorology* 151(12):1622–31.

Risk D, Nickerson N, Phillips CL, Kellman L, Moroni M. 2012. Drought alters respired $\delta^{13}CO_2$ from autotrophic, but not heterotrophic soil respiration. *Soil Biology and Biochemistry* 50:26–2.

Schuur EAG, Trumbore SE. 2006. Partitioning sources of soil respiration in boreal black spruce forest using radiocarbon. *Global Change Biology* 12(2):165–76.

Singh B, Nordgren A, Lofvenius MO, Högberg MN, Mellander P-E, Högberg P. 2003. Tree root and soil heterotrophic respiration as revealed by girdling of boreal Scots pine forest: extending observations beyond the first year. *Plant, Cell and Environment* 26(8):1287–96.

Southon JR. 2011. Are the fractionation corrections correct: Are the isotopic shifts for $^{14}C/^{12}C$ ratios in physical processes and chemical reactions really twice those for $^{13}C/^{12}C$? *Radiocarbon* 53(4):691–704.

Stuiver M, Polach HA. 1977. Discussion: reporting of ^{14}C data. *Radiocarbon* 19(3):355–63.

Trumbore S. 2000. Age of soil organic matter and soil respiration: radiocarbon constraints on belowground C dynamics. *Ecological Applications* 10(2):399–11.

Trumbore S. 2006. Carbon respired by terrestrial ecosystems – recent progress and challenges. *Global Change Biology* 12(2):141–53.

Venterea RT, Baker JM. 2008. Effects of soil physical nonuniformity on chamber-based gas flux estimates. *Soil Science Society of America Journal* 72(5):1410–7.

Wang Y, Amundson R, Trumbore S. 1994. A model for soil $^{14}CO_2$ and its implications for using ^{14}C to date pedogenic carbonate. *Geochimica et Cosmochimica Acta* 58(1):393–9.

https://doi.org/10.2458/56.17771 Published online by Cambridge University Press